Applied Entomology and Zoology (2019) 54:389–398
https://doi.org/10.1007/s13355-019-00635-z

ORIGINAL RESEARCH PAPER

Characterization of the channel-pores formed by *Bacillus thuringiensis* Cry46Ab toxin in planar lipid bilayers

Akira Sakakibara[1] · So Takebe[2] · Toru Ide[1] · Tohru Hayakawa[1]

Received: 28 January 2019 / Accepted: 5 August 2019 / Published online: 16 August 2019

Abstract

Cry46Ab from *Bacillus thuringiensis* TK-E6 is a new mosquitocidal toxin with aerolysin-type architecture, and has been shown that co-administration of Cry46Ab with other mosquitocidal Cry toxins results in synergistic toxicity against *Culex pipiens* Coquillett (Diptera: Culicidae) mosquito larvae. Cry46Ab, therefore, is expected to find use in improving the insecticidal activity of *B. thuringiensis*-based bioinsecticides. In the present study, the mode of action of Cry46Ab was explored by single-channel measurements of Cry46Ab channel-pores. The single-channel conductances of channel-pores formed in planar lipid bilayers by Cry46Ab were determined to be 31.8 ± 2.7 pS in 150 mM NaCl and 24.2 ± 0.7 pS in 150 mM $CaCl_2$. Ion-selectivity measurements revealed that the channel-pores formed by Cry46Ab were cation selective. The permeability ratio of K^+ to Cl^- was approximately 4, and the preferences for cations were $K^+ > Na^+$, $K^+ > Ca^{2+}$, and $Ca^{2+} > Na^+$. A calcein release assay using liposomes suggested that Cry46Ab influences the integrity of membrane vesicles. Formation of cation-selective channel-pores has been observed with other insecticidal Cry toxins that have structures distinct from those of Cry46Ab; the capability of forming such pores may be a property required of insecticidal toxins.

Keywords *Bacillus thuringiensis* · Cry46Ab toxin · Planar lipid bilayer · Single-channel analysis · Calcein release assay

Introduction

Mosquito control is a central means by which mosquito-borne diseases such as malaria, viral hemorrhagic fever, and lymphatic filariasis can be prevented. Chemical insecticides have traditionally been used for mosquito control, but these agents have negative impacts on other organisms and the environment. These concerns, therefore, have prompted the development of alternative approaches such as biological control. The gram-positive spore-forming bacterium *Bacillus thuringiensis* subsp. *israelensis* (Bti) shows strong toxicity against *Anopheles*, *Aedes*, and *Culex* mosquito larvae, and is one of the most widespread and environmentally friendly components used in materials employed for mosquito control. The mosquitocidal activity of Bti resides in three major Cry toxins (Cry4Aa, Cry4Ba, and Cry11Aa) and a Cyt toxin (Cyt1Aa). The structures of Bti Cry toxins have been shown to share a similar three-domain architecture (domains I, II, and III) (Boonserm et al. 2005, 2006; de Maagd et al. 2001). On the other hand, Cyt1Aa has a single domain with a β-sheet in the center surrounded by two α-helical layers (Cohen et al. 2011). Cyt1Aa has a low mosquitocidal activity, but this Cyt toxin synergizes with the Cry toxins (Crickmore et al. 1995; Pérez et al. 2005; Wirth et al. 1997, 2005; Wu et al. 1994). Surprisingly, although Bti-based bioinsecticides have been used to control mosquitos for many years, resistance to the bioinsecticides has not yet been reported in field populations of mosquitoes (Ben-Dov 2014). The lack of resistance to Bti-based bioinsecticides has been attributed primarily to the different modes of action of, and synergistic interactions among, Bti toxins (Crickmore et al. 1995; Poncet et al. 1995; Wirth et al. 2005). However, application of insecticides is always accompanied by the risk of selecting insecticide resistance in larval mosquito populations; thus, it is possible that mosquitoes may develop resistance to Bti-based bioinsecticides in the future, as has been reported in field populations of lepidopteran insects

✉ Tohru Hayakawa
hayaka-t@cc.okayama-u.ac.jp

[1] Graduate School of Interdisciplinary Science and Engineering in Health Systems, Okayama University, 3-1-1 Tsushima-naka, Kita-ku, Okayama 700-8530, Japan

[2] Graduate School of Biology-Oriented Science and Technology, Kindai University, 930 Nishimitani, Kinokawa 649-6493, Japan

(Tabashnik et al. 1990). In fact, it has been shown in the laboratory that heavy and continuous application of individual Bti-derived Cry toxins can induce resistance (Georghiou and Wirth 1997; Wirth et al. 2012). It is, therefore, desirable to find toxins with modes of action that differ from those of Bti toxins to prolong the useful life of Bti-based bioinsecticides.

Cry46Ab is a crystal protein derived from *B. thuringiensis* strain TK-E6. Upon activation by proteinase K, Cry46Ab shows high cytotoxicities to human leukemic T cells (MOLT-4 and Jurkat), but not to human embryonal kidney cells (HEK293) (Hayakawa et al. 2007). Cry46Ab is, therefore, named parasporin 2Ab exhibiting preferential cytotoxicity against human cancer cells by Committee of Parasporin Classification and Nomenclature (http://parasporin.fitc.pref.fukuoka.jp/index.html). On the other hand, it has recently been reported that Cry46Ab shows apparent toxicity against *Culex pipiens* Coquillett (Diptera: Culicidae) mosquito larvae (Hayakawa et al. 2017). Toxicity spectra of Cry46Ab other than human leukemic T cells and *C. pipiens* mosquito larvae remains to be elucidate.

Interestingly, co-administration of Cry46Ab with other mosquitocidal Cry toxins, especially the combination of Cry46Ab with Cry4Aa from Bti, results in significant synergistic toxicity against *C. pipiens* mosquito larvae (Hayakawa et al. 2017). Cry46Ab thus may be a good candidate to improve the activity of crystal toxin insecticides currently in use, and may prolong the life of Bti-based bioinsecticides. Cry46Ab shows highest homology (84% identity at the amino acid sequence level) to Cry46Aa, a toxin that also is referred to as parasporin-2Aa, from *B. thuringiensis* strain A1547 (Ito et al. 2004). Cry46Ab also shows relatively high homology (approximately 40% identity at the amino acid sequence level) to hydralysin, a toxin produced by the green hydra *Chlorohydra viridissima* (Sher et al. 2005). Therefore, Cry46Ab is inferred to be a member of the aerolysin-type β pore-forming toxins, a family that includes parasporin-2Aa and hydralysin. In general, aerolysin-type toxins are produced by a very diverse group of organisms, and this large family of toxins contains not only aerolysins from *Aeromonas hydrophila* and related *Aeromonas* species, but also epsilon toxin from *Clostridium perfringens*, alpha toxin from *C. septicum*, enterolobin from *Enterolobium contortisiliquum* (a Brazilian tree), and Mtx toxin from *Lysinibacillus sphaericus* (Knapp et al. 2010). Aerolysin-type toxins share structural similarities in their domains, and all act as cytolysins via pore formation. On the other hand, Cry toxins can be divided into several distinct homology groups (Schnepf et al. 1998), and most of them (nearly 90%) belongs to the three-domain Cry toxin group (see http://www.lifesci.sussex.ac.uk/home/Neil_Crickmore/Bt/). The three-domain Cry toxin is a member of the α pore-forming toxin which employ α-helices to insert into the membrane, and are believed to form cation-selective channel-pores (Xu et al. 2014).

Cry46Ab is a functional pore-forming toxin with the single-channel conductance of 103.3 ± 4.1 pS (mean ± standard deviation) in 150 mM KCl (Hayakawa et al. 2017), but other characteristics of Cry46Ab channel-pores remain unclear. In the present study, the mode of action of channel-pores formed by Cry46Ab was further analyzed using planar lipid bilayers and liposomes.

Materials and methods

Preparation of recombinant Cry46Ab toxin

Recombinant Cry46Ab fused with glutathione *S*-transferase (GST-Cry46Ab) was expressed in *Escherichia coli* BL21 as described previously (Hayakawa et al. 2017). Briefly, *E. coli* cells harboring pGST-Cry46Ab-S1 (Hayakawa et al. 2017) were cultured at 37 °C in TB medium containing ampicillin (100 μg/ml) until the optical density at 600 nm (OD_{600}) reached 0.4–0.6, and then expression of recombinant Cry46Ab was induced with 0.1 mM isopropyl β-D-1-thiogalactopyranoside at 30 °C for 4 h. The GST-Cry46Ab was purified using glutathione-Sepharose 4B (GE Healthcare Bio-Sciences AB, Uppsala, Sweden) according to the manufacturer's instructions. Protein concentration was estimated using a protein assay kit (Bio-Rad Laboratories, Inc., Hercules, CA), with bovine serum albumin as the standard. The mosquito-larvicidal activity of the GST-Cry46Ab was analyzed by bioassay using *C. pipiens* larvae (3rd instar), as described previously (Hayakawa et al. 2017). Briefly, 40 μg of the GST-Cry46Ab was adsorbed onto 2 mg of latex beads (0.8 μm diameter, Sigma-Aldrich Corp., St. Louis, MO), and then administered to the mosquito larvae as a diet. In a preliminary experiment, latex beads adsorbed GST was not toxic against *C. pipiens* larvae at a working concentration of 2 μg/ml (data not shown).

Purified GST-Cry46Ab was activated using a trypsin-immobilized column as described previously (Hayakawa et al. 2017). The activation process was monitored by analysis using sodium dodecyl sulfate—15% polyacrylamide gel electrophoresis (SDS-PAGE), and the activated Cry46Ab (a polypeptide of 29 kDa) was eluted as the flow-through. Activated Cry46Ab was concentrated using Vivaspin 20 (10 kDa molecular weight cutoff) centrifugal filter devices (GE Healthcare Bio-Sciences AB).

Lipid bilayer experiments

Pore formation by activated Cry46Ab in planar lipid bilayers was analyzed as described previously (Hayakawa et al. 2017). Briefly, each instrument consisted of two chambers (upper, *cis* chamber; lower, *trans* chamber), and the bottom of the *cis* chamber was a thin sheet of polyvinyl chloride

with a small circular hole (approximately φ200 µm). A lipid bilayer was prepared by painting an asolectin (phospholipids from soybean, Sigma-Aldrich Corp.) solution (40 mg/ml n-decane) across the small hole. The chambers were held at virtual ground, such that the voltage in the solution of the *cis* chamber was connected to a patch-clamp amplifier by an Ag/AgCl electrode-defined membrane potential. After injection of activated Cry46Ab (0.1 µg/ml) into the solution in the *cis* chamber, the toxin was incorporated into the lipid bilayer while applying a 70 mV holding potential across the lipid bilayer. Data were analyzed using pClamp software (ver 9.2, Axon Instruments, Foster City, CA).

Unless otherwise stated, the current amplitude of the resolvable steps was recorded for each experiment, and the resulting data were plotted versus the corresponding applied voltage to generate the current–voltage relationship. Channel conductance was determined from the slope of the linear regressions on similar data points. Corresponding values obtained in different experiments were subjected to descriptive analysis by calculating (over the number of experiments in which the values had been observed) the arithmetic mean and standard deviation.

To assess ion selectivity of the pores formed by Cry46Ab, membrane currents through the channel-pore formed by Cry46Ab were recorded with a fourfold gradient of KCl across the lipid bilayer (600 mM KCl and 10 mM Tris–HCl (pH 8.0) in the *cis* chamber, 150 mM KCl and 10 mM Tris–HCl (pH 8.0) in the *trans* chamber). The zero-current reversal potential (V_R) was obtained as X-intercept of the linear showing current–voltage relationship, and the P_K/P_{Cl} permeability ratio was calculated using the Goldman–Hodgkin–Katz equation as follows (Benz et al. 1979).

$$V_R = \frac{RT}{F} \mathrm{In} \frac{P_K [K^+]_{cis} + P_{Cl}[Cl^-]_{trans}}{P_K [K^+]_{trans} + P_{Cl}[Cl^-]_{cis}}$$

In the formula, R is the molar gas constant, T is the absolute temperature, and F is the Faraday constant.

Calcein release assay

Large unilamellar vesicles (LUVs) of liposome were prepared as described previously (Shai et al. 1990) with some modifications. Briefly, 5 mg of asolectin (Sigma-Aldrich Corp.) was dissolved in 500 µl of chloroform. The chloroform then was removed using a circulating aspirator to generate a thin film of asolectin. The film was suspended in 500 µl of calcein solution (100 mM calcein, 100 mM NaCl, and 50 mM Tris–HCl, pH 8.3) by sonication for 10 min at intervals of 30 s on, 30 s off. The resulting suspension was allowed to stand for 30 min at room temperature to permit the formation of multilamellar vesicles, leading in turn to the subsequent formation of small unilamellar vesicles of liposome. Liposomal LUVs were generated by subjecting the small unilamellar vesicle suspension to repeated freeze–thaw cycles using liquid nitrogen at room temperature. LUVs containing calcein were purified using discontinuous sucrose density gradient centrifugation. The sucrose gradient was generated by sequential layering of 35, 30, 25, 20, and 10% (*w*/*w*) sucrose solutions. The liposome suspension was mixed with two volumes of 64% (*w*/*w*) sucrose to yield a suspension in a solution of approximately 40% (*w*/*w*) sucrose, and this mixture was placed at the bottom of sucrose gradient. After centrifugation at 200,000×*g* for 1.5 h at 4 °C, the thin orange-colored layer of the liposome fraction was collected; the orange color indicated the presence of self-quenched calcein. The liposomes then were subjected to a second round of purification using sucrose density gradient centrifugation (for two purifications total).

The ability of Cry46Ab to disrupt liposomes was evaluated by a calcein release assay. Calcein is self-quenched at high concentration (100 mM), as in the liposome, but emits fluorescence when calcein is diluted by disruption of the liposome. The fluorescence intensity of calcein released from the liposomes was measured using a spectrofluorophotometer (RF-5300pc, Shimadzu, Osaka, Japan) with excitation at 490 nm and emission at 520 nm. Fluorescence intensity was monitored every 20 s for 5 min after addition of the activated Cry46Ab to the liposome suspension. The amount of fluorescence released was expressed as a percentage of the maximum fluorescence intensity achieved by the addition of Triton X-100 at a final concentration of 1% which disrupts liposome completely (fluorescence recovery).

Results

Recombinant Cry46Ab

Recombinant Cry46Ab was successfully expressed as a GST fusion in *E. coli*, and the molecular mass of purified GST-Cry46Ab was approximately 60 kDa, similar to the expected mass (59.309 kDa) (Fig. 1a). After treatment using a trypsin-immobilized column, GST-Cry46Ab was processed into a polypeptide of 29 kDa (Fig. 1a), similar in size to that of the activated Cry46Ab that was shown to be toxic against human leukemic T cells (Hayakawa et al. 2007) and against *C. pipiens* larvae (Hayakawa et al. 2017). GST-Cry46Ab exhibited apparent toxicity against *C. pipiens* larvae, with an LC_{50} value (95% confidence limits) of 1.01 (0.98–1.05) µg/ml (Fig. 1b).

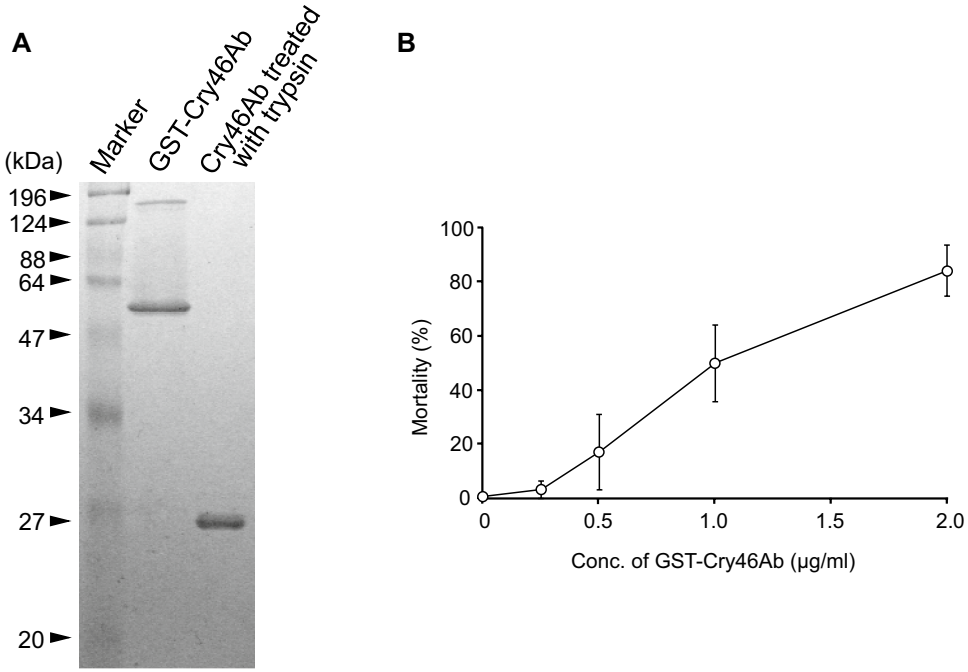

Fig. 1 The recombinant Cry46Ab toxin. **a** The recombinant Cry46Ab expressed as a GST fusion was purified using glutathione beads, and was activated using a trypsin-immobilized column. Protein was analyzed by 15% SDS-PAGE. A total of 1 μg of protein was applied in each lane. **b** Mosquitocidal activities of GST-Cry46Ab. The experiments were repeated independently six times. Mortality rates, observed at 48 h after administration, are presented as mean (standard deviation)

Single-channel measurement

Pore formation by activated Cry46Ab in the planar lipid bilayer was assessed previously, when the single-channel conductance was determined to be 103.3 ± 4.1 pS in 150 mM KCl (Hayakawa et al. 2017). In the present study, to characterize more precisely the channel-pores formed by Cry46Ab in a planar lipid bilayer, the ability of Cry46Ab to permeabilize an artificial lipid bilayer was analyzed in salt solutions containing NaCl or $CaCl_2$, salts distinct from the KCl used in the previous experiments.

In a symmetrical salt solution containing 150 mM NaCl and 10 mM Tris–HCl (pH 8.0), apparent channel currents were detected between − 100 and + 100 mV at approximately 30 min after the addition of activated Cry46Ab to the solution in the *cis* chamber (Fig. 2a). These channel currents were observed only in the presence of toxin. The recordings of membrane currents were similar to those observed previously in 150 mM KCl (Hayakawa et al. 2017), and were characterized as long periods of closure interrupted by bursts of current jumps and rapid flickering between open and closed states (Fig. 2a). The current–voltage relationship was linear at several conductance levels. Most frequently observed was a line indicating a channel conductance of 31.8 ± 2.7 pS, followed (successively less frequently) by lines indicating conductances of 59.7 ± 1.1, 89.8 ± 0.7, 119.4 ± 1.3 and 150.6 ± 2.8 pS (Fig. 2b, c). In fact, 639 single events were recorded in total, consisting of 259, 127, 82, 76, and 34 events at the respective channel conductances (Fig. 2b, c). As the channel conductances observed in this experiment occurred almost universally in multiples of approximately 30 pS, channel conductance higher than 30 pS was considered to be the result of the synchronized opening and closing of multiple channels. The conductance of single channels formed by Cry46Ab on the planar lipid bilayer thus was determined to be 31.8 ± 2.7 pS in 150 mM NaCl.

Recordings of membrane currents in the solution containing 150 mM $CaCl_2$ and 10 mM Tris–HCl (pH 8.0) yielded a profile similar to those observed in KCl and NaCl solutions (Fig. 3a). In the current–voltage relationship, the most frequently observed line was one indicating a channel conductance of 24.2 ± 0.7 pS (Fig. 3b, c). Although the frequency was low, a line indicating a conductance of 52.6 ± 3.9 pS also was observed (Fig. 3b, c). Three hundred and sixty-four single events were recorded in total, and 230 and 71 of the events occurred on lines indicating channel conductances of 24.2 ± 0.7 and 52.6 ± 3.9 pS, respectively (Fig. 3b, c). Thus, the conductance of single channels formed by Cry46Ab on the planar lipid bilayer was determined to be 24.2 ± 0.7 pS in 150 mM $CaCl_2$.

Ion selectivity of the pores formed by Cry46Ab

Membrane currents through the channel-pore formed by Cry46Ab also were recorded with a fourfold gradient of KCl across the lipid bilayer. As a result, various channel currents with different levels were detected between − 50 and + 50 mV upon addition of activated Cry46Ab to the solution in the *cis* chamber (data not shown). In this assay, the current amplitudes of the resolvable steps were recorded, pooled for eight independent experiments, and averaged over

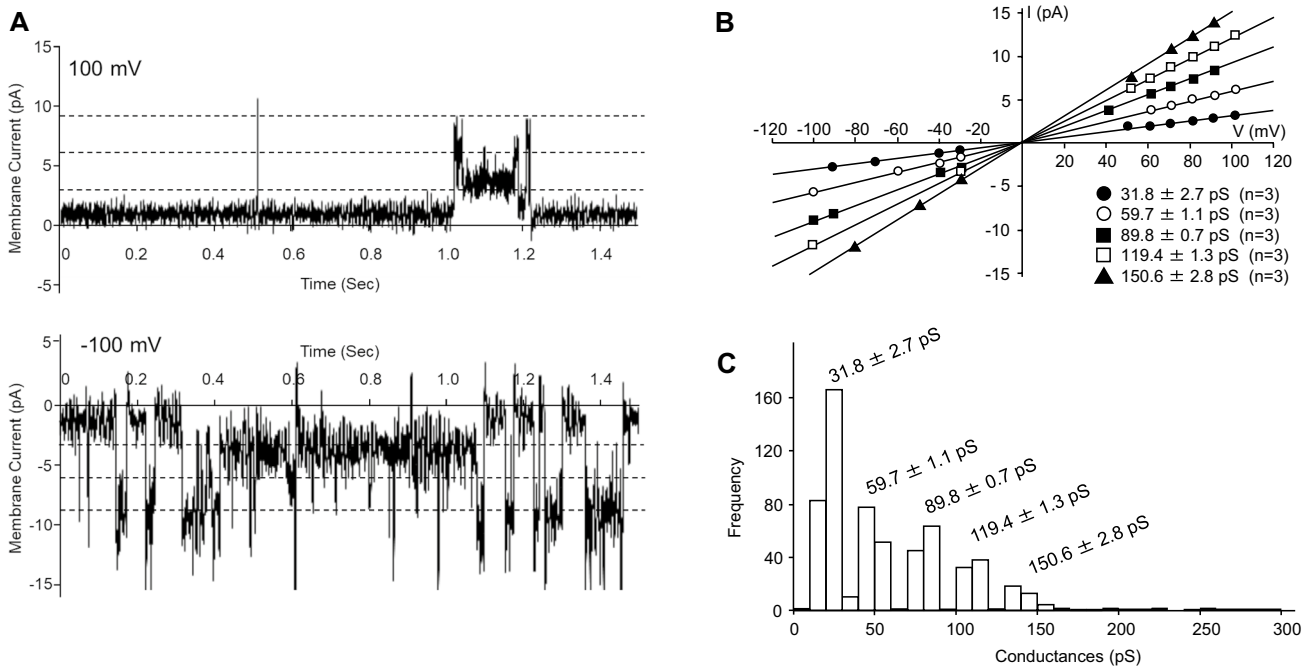

Fig. 2 Single-channel analysis of activated Cry46Ab in symmetrical 150 mM NaCl solutions. **a** Representative segments of typical current traces. The current levels corresponding to the open state of the channels are indicated by dashed lines. **b** Representative current–voltage relationship obtained from the Cry46Ab current steps. The experiment was repeated three times independently, and the mean and standard deviation is shown. **c** Frequency of conductance observed on the Cry46Ab current steps. Six hundred and thirty-nine single events were recorded in total

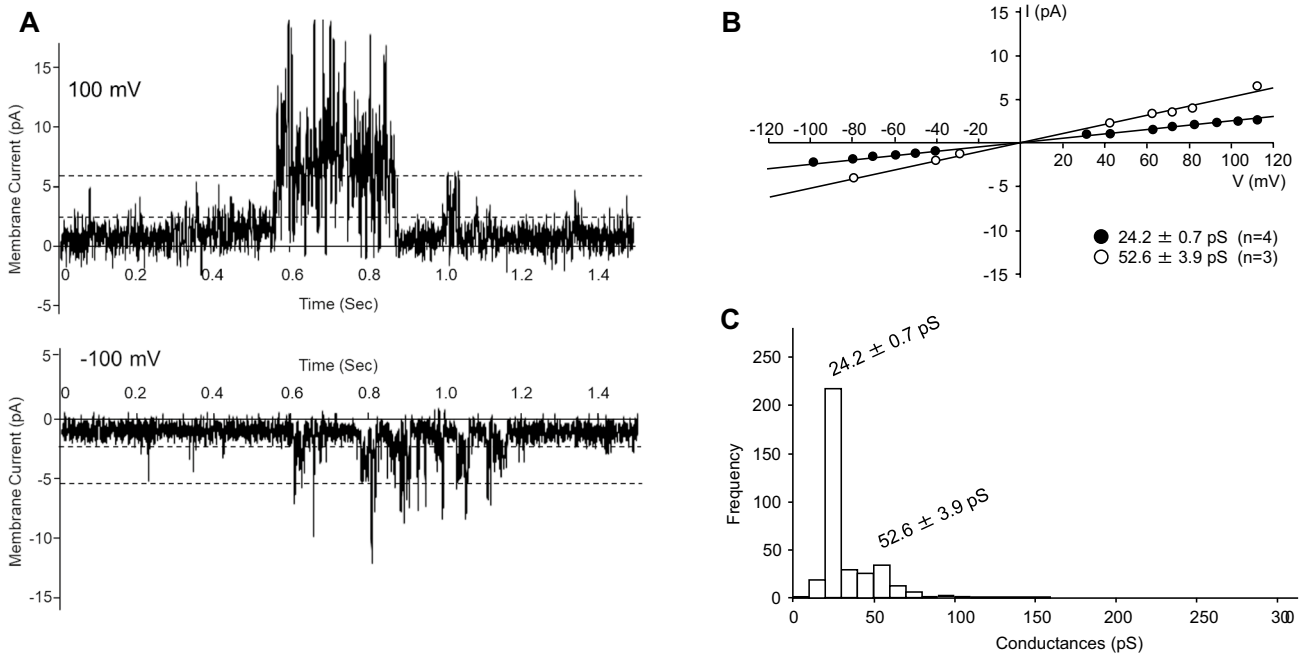

Fig. 3 Single-channel analysis of activated Cry46Ab in symmetrical 150 mM $CaCl_2$ solutions. **a** Representative segments of typical current traces. The current levels corresponding to the open state of the channels are indicated by dashed lines. **b** Representative current–voltage relationship obtained from the Cry46Ab current steps. The experiment was repeated more than three times independently, and the mean and standard deviation are shown. **c** Frequency of conductance observed on the Cry46Ab current steps. Three hundred and sixty-four single events were recorded in total

the number of steps at each applied voltage (Fig. 4a). Considering the results of single-channel measurements in this study and in the previous report (Hayakawa et al. 2017), Cry46Ab is thought to form channel-pores with very similar conductances in planar lipid bilayers, and higher channel currents are thought to be caused by synchronized opening and closing of multiple channels. It was, therefore, reasonable to speculate that all of the linear showing current–voltage relationship observed in the present experiment share the same X-intercept. In fact, the current–voltage relationship constructed for this measurement approached linearity, and the V_R was determined to be − 18.38 mV (Fig. 4a). The P_K/P_{Cl} permeability ratio calculated from this V_R value (using the Goldman–Hodgkin–Katz equation (Benz et al. 1979)) was 3.67, demonstrating a higher permeability for K^+ than for Cl^-.

In addition, the effect of pH on the channel-pore formed by Cry46Ab was assessed. The membrane currents were recorded under the same experimental conditions as above, but 10 mM Tris–HCl (pH 6.0) was used as the buffer instead of 10 mM Tris–HCl (pH 8.0). As a result, various channel currents were detected at voltages between − 50 and + 50 mV, with these currents occurring at levels distinct from those observed in the measurement using a buffer of pH 8.0 (data not shown). The current amplitudes of the resolvable steps were recorded, pooled for seven independent experiments, and averaged over the number of steps at each applied voltage. The current–voltage relationship approached linearity, and the V_R was determined to be − 20.04 mV; the P_K/P_{Cl} permeability ratio calculated from this V_R value was 4.25 (Fig. 4b). Thus, the channel-pores formed in the planar lipid bilayer by Cry46Ab appear to be cation selective.

Preferred cations

To determine the preferred cations (K^+, Na^+, or Ca^{2+}) for the channel-pores formed by Cry46Ab, membrane currents were measured across the lipid bilayer when different salt solutions were present on the two sides of the chamber. In this experiment, KCl and NaCl were used at a concentration of 150 mM, and $CaCl_2$ was used at a concentration of 75 mM to provide Cl^- at a concentration equivalent to those in the KCl and NaCl solutions.

When 150 mM KCl was provided in the *cis* chamber and 150 mM NaCl was provided in the *trans* chamber, incorporation of Cry46Ab into the lipid bilayer yielded positive membrane current without holding potential (Fig. 5a). Similar preferential permeability was observed when the salt solutions were exchanged between the *cis* and *trans* chambers (150 mM NaCl in the *cis* chamber and 150 mM KCl in the *trans* chamber) (Fig. 5b). This result demonstrated that the Cry46Ab channel-pore has a higher permeability for K^+ than for Na^+, and that the movement of K^+ across the lipid bilayer occurs in both directions through this channel-pore. On the other hand, when the measurement was performed with 150 mM KCl in the *cis* chamber and 75 mM $CaCl_2$ in the *trans* chamber, positive membrane current was observed (Fig. 5c), indicating preferential permeability for K^+ compared to Ca^{2+}. When the measurement was performed with 150 mM NaCl in the *cis* chamber and 75 mM $CaCl_2$ in the *trans* chamber, negative membrane current was observed (Fig. 5d), indicating preferential permeability for Ca^{2+} compared to Na^+. Therefore, the cation preferences of the channel-pores formed by Cry46Ab were $K^+ > Na^+$, $K^+ > Ca^{2+}$, and $Ca^{2+} > Na^+$.

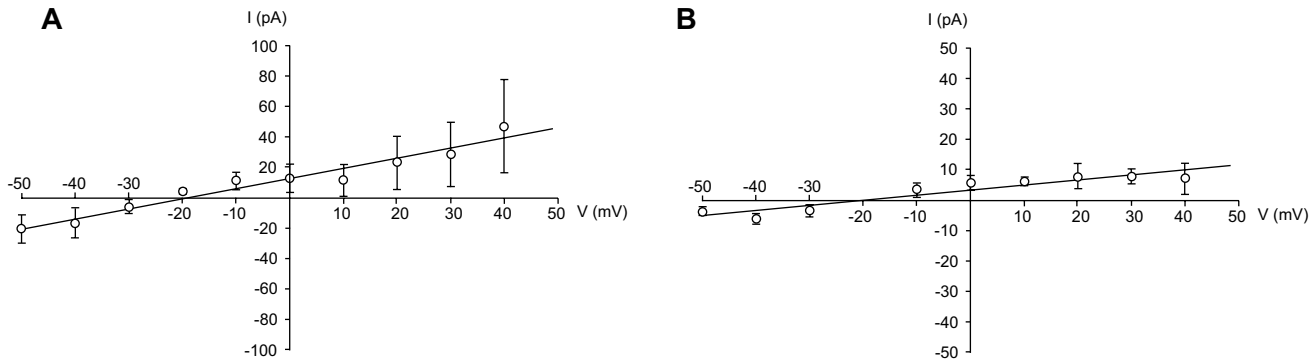

Fig. 4 Ion selectivity of the channel-pore formed by activated Cry46Ab. Anion–cation selectivity of the channel-pore was determined using fourfold gradients of KCl across the lipid bilayer. Current amplitudes of the resolvable steps were recorded, pooled for eight independent experiments, and averaged over the number of steps at each applied voltage. The current–voltage relationship was constructed and the zero-current reversal potential (V_R) was determined. The P_K/P_{Cl} permeability ratios were calculated from this V_R value using the Goldman–Hodgkin–Katz equation. **a** Measurement in pH 8.0 solution. **b** Measurement in pH 6.0 solution

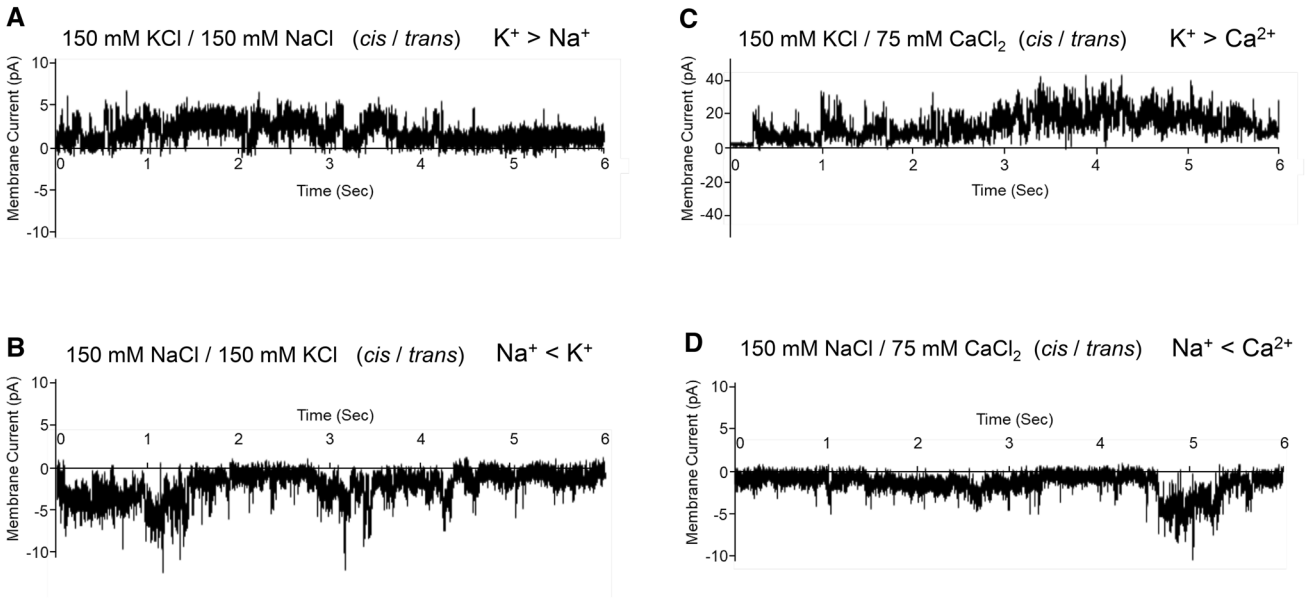

Fig. 5 Selectivity order of cations for the channel-pore formed by activated Cry46Ab. Selectivity order of cations for the channel-pore formed by activated Cry46Ab was determined by membrane current measurement under asymmetrical buffer conditions using **a** 150 mM KCl/150 mM NaCl, **b** 150 mM NaCl/150 mM KCl, **c** 150 mM KCl/75 mM $CaCl_2$, **d** 150 mM NaCl/75 mM $CaCl_2$ (*cis* chamber/*trans* chamber), respectively. Membrane current was measured without holding potential upon incorporation of Cry46Ab into the lipid bilayer

Calcein release assay

LUVs of asolectin were created with the self-quenched fluorescent dye calcein entrapped in their interior cavities, and membrane perturbation was monitored by the increase in fluorescence due to the dilution of calcein in the surrounding solution. After addition of activated Cry46Ab to the LUV suspension, the fluorescence intensity increased in a rapid and dose-dependent manner (Fig. 6). The estimated fluorescence recoveries at 5 min after addition of Cry46Ab at 10.0, 2.5, and 0.6 µg/ml (final concentration) were 59.2, 46.2, and 15.9%, respectively (Fig. 6). These observations suggested that Cry46Ab (and presumably, the channel-pore formed by Cry46Ab) influences the integrity of membrane vesicles.

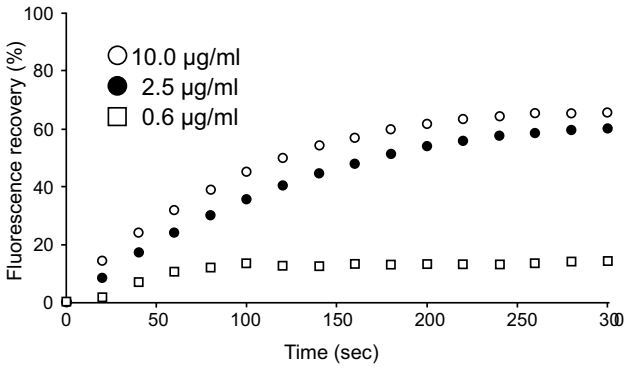

Fig. 6 Calcein release assay. LUVs of asolectin were created with the self-quenched fluorescent dye calcein entrapped in their interior cavities. After addition of activated Cry46Ab to the LUV suspension, the increase in fluorescence intensity was monitored every 20 s for 5 min. Fluorescence recovery was expressed as a percentage of the maximum fluorescence intensity, achieved by the addition of Triton X-100. Open circles (○), filled circles (●) and squares indicate final concentration of Cry46Ab at 10.0, 2.5, and 0.6 µg/ml, respectively

Discussion

We previously demonstrated that Cry46Ab is a functional pore-forming toxin with a single-channel conductance of 103.3 ± 4.1 pS in 150 mM KCl (Hayakawa et al. 2017), but other characteristics of these channel-pores remained unclear. Therefore, to characterize the channel-pore more precisely, single-channel analyses were performed using NaCl or $CaCl_2$ solution, that is, employing salts distinct from the previously tested KCl. The measurements of membrane currents in both 150 mM NaCl and 150 mM $CaCl_2$ solutions revealed typical current transitions between open and closed states, and a result similar to that previously observed in the 150 mM KCl solution. Single-channel conductances of the channel-pores in 150 mM NaCl and in 150 mM $CaCl_2$ were 31.8 ± 2.7 and 24.2 ± 0.7 pS, respectively. However, the single-channel conductance of the channel-pore in 150 mM NaCl was apparently lower than that in 150 mM KCl; this observation may suggest some difference in characteristics of the Cry46Ab channel-pores compared to those formed by

aerolysin. Notably, aerolysin from *S. sobria* has been shown to form channel-pores with similar single-channel conductance in both KCl and NaCl solutions (650 pS in 1 M KCl; 600 pS in 1 M NaCl) (Chakraborty et al. 1990).

Measurement of membrane currents in a fourfold KCl gradient (600 mM in the *cis* chamber, 150 mM in the *trans* chamber) demonstrated that the channel-pores formed by Cry46Ab permeabilized K^+ in preference to Cl^-; the P_K/P_{Cl} permeability ratios calculated at pH 6.0 and 8.0 were 3.67 and 4.25, respectively. The cation preference of the Cry46Ab channel-pores were determined to be $K^+ > Na^+$, $K^+ > Ca^{2+}$, and $Ca^{2+} > Na^+$. Formation of cation-selective channel-pores in planar lipid bilayers has been observed with other insecticidal Cry toxins, including Cry1Aa (Grochulski et al. 1995), Cry1Ac (Slatin et al. 1990), Cry1C (Schwartz et al. 1993), Cry3Aa (Slatin et al. 1990), Cry3B2 (Von Tersch et al. 1994), and Cry4Ba (Puntheeranurak et al. 2004). Like Cry46Ab, these molecules are insecticidal Cry toxins, but unlike Cry46Ab, these other toxins are members of the α pore-forming toxin family and do not share structural similarity with aerolysin-type toxins. It is believed that, after sequential interaction with specific receptors facilitating formation of the toxin oligomer, insecticidal Cry toxins insert into the cell membrane of columnar cells in the midgut tissue and create pores that allow cell uptake of cations. The uptake of cations causes the influx of excess water into the midgut cells, leading to swelling and bursting, a cell lysis process referred to as colloid-osmotic lysis (Knowles and Ellar 1987). Considering this previous work and the observations in the present work, the formation of cation-selective channel-pores by crystal proteins may be a property required of insecticidal toxins. In the present study, the effect of channel-pores formed by Cry46Ab on the integrity of membrane vesicles also was assessed by the calcein release assay. After addition of activated Cry46Ab to LUVs containing self-quenched calcein, fluorescence intensity increased quickly in a dose-dependent manner. This observation suggested that Cry46Ab, and presumably the channel-pore formed by Cry46Ab, influences the integrity of membrane vesicles.

On the other hand, among aerolysin-type toxins, the enterotoxin from *C. perfringens* forms highly cation-selective channel-pores in planar lipid bilayers (Benz and Popoff 2018), but other aerolysin-type toxins [including aerolysin from *A. sobria* (Chakraborty et al. 1990)], alpha toxin from *C. septicum* (Ballard et al. 1993), and epsilon toxin from *C. perfringens* (Petit et al. 2001)) form slightly anion-selective channel-pores in planar lipid bilayers. All these aerolysin-type toxins are classified as β pore-forming toxins that, upon binding to the receptor of the target cell, form toxin oligomers that can insert into the cell membrane and form channel-pores. Formation of channel-pores induces ion fluxes leading to membrane depolarization and ultimately cell death (Abrami et al. 2000). The amphipathic β-hairpin in the middle domain of these toxin molecules is thought to constitute the transmembrane β-barrel cylinder (Melton et al. 2004). The β-hairpin is composed of a striking pattern of alternating charged and non-charged amino acids; the charged amino acids are thought to line the lumen of the β-barrel cylinder (Melton et al. 2004). It is believed that the composition and/or sequence of charged amino acids in the β-hairpin region is responsible for the ion selectivity of aerolysin-type toxins. The corresponding β-hairpin can be identified in the structure of Cry46Ab based on its sequence similarity with Cry46Aa (parasporin-2Aa, Akiba et al. 2009). Therefore, it will be of interest to determine the amino acid residues in the β-hairpin of Cry46Ab that affect the ion selectivity, as well as the effect of this domain on to Cry46Ab's insecticidal activity. Currently, the residues that determine the ion selectivity of channel-pores remain unclear; Cry46Ab may be useful as a model for elucidating the mechanism of ions permeation through such channel-pores.

Co-administration of Cry46Ab with other mosquitocidal Cry toxins (including Cry4Aa, Cry11Aa, and Cry11Ba) has been shown to result in synergistic toxicity against *C. pipiens* mosquito larvae (Hayakawa et al. 2017). Cry4Aa (Boonserm et al. 2006), Cry11Aa (Fernández et al. 2005), and Cry11Ba (Likitvivatanavong et al. 2009) are three-domain Cry toxin, and are, therefore, hypothesized to form cation-selective channel-pores in a manner similar to that of other insecticidal Cry toxins. On the other hand, it is unclear whether this synergistic toxicity is generated in association with the cation-selective channel-pore formation. Specifically, it is possible that the mechanism of this synergistic toxicity depends on multiple other factors in addition to pore formation.

It is widely accepted that Cry toxin recognizes the specific receptors on midgut epithelial cells of susceptible insect larva. The specific receptors promote toxin-membrane interaction, and are believed to play a crucial role in the insecticidal spectra. Since Cry46Ab also exhibits specificity, a specific receptor should be present on the target cell membrane. On the other hand, formation of channel-pores is probably a fundamental property of Cry toxins, it is believed that Cry toxins at high concentration is able to form channel-pores in a membrane even without specific receptors. In fact, it has been demonstrated that several Cry toxins form channel-pores in the planar lipid bilayer without specific receptors (Grochulski et al. 1995; Puntheeranurak et al. 2004; Schwartz et al. 1993; Slatin et al. 1990; Von Tersch et al. 1994). In the present study, we used 0.1 μg/ml of Cry46Ab for single-channel measurements, and the concentration was demonstrated to be high enough to form channel-pores in planar lipid bilayer. On the other hand, calcein release assay revealed that much higher concentration of Cry46Ab (> 0.6 μg/ml) required to influence the integrity

of membrane vesicles. It is speculated that if the membrane with specific receptors is available, amount of Cry46Ab required for measurements is reduced. It is plausible to conclude that the channel-pores observed in the present study are central to the toxicity of Cry46Ab.

Acknowledgements *C. pipiens* eggs were kindly supplied by the Research and Development Laboratory at Dainihon Jochugiku Co., Ltd., Osaka, Japan. This work was supported in part by JSPS KAKENHI Grant number JP18K05675.

References

Abrami L, Fivaz M, van der Goot FG (2000) Adventures of a pore-forming toxin at the target cell surface. Trends Microbiol 8:168–172. https://doi.org/10.1016/S0966-842X(00)01722-4

Akiba T, Abe Y, Kitada S, Kusaka Y, Ito A, Ichimatsu T, Katayama H, Akao T, Higuchi K, Mizuki E, Ohba M, Kanai R, Harata K (2009) Crystal structure of the parasporin-2 *Bacillus thuringiensis* toxin that recognizes cancer cells. J Mol Biol 386:121–133. https://doi.org/10.1016/j.jmb.2008.12.002

Ballard J, Sokolov Y, Yuan WL, Kagan BL, Tweten RK (1993) Activation and mechanism of *Clostridium septicum* alpha toxin. Mol Microbiol 10:627–634. https://doi.org/10.1111/j.1365-2958.1993.tb00934.x

Ben-Dov E (2014) *Bacillus thuringiensis* subsp. *israelensis* and its dipteran-specific toxins. Toxins 6:1222–1243. https://doi.org/10.3390/toxins6041222

Benz R, Popoff MR (2018) *Clostridium perfringens* enterotoxin: the toxin forms highly cation-selective channels in lipid bilayers. Toxins (Basel) 10:E341. https://doi.org/10.3390/toxins10090341

Benz R, Janko K, Läuger P (1979) Ionic selectivity of pores formed by the matrix protein (Porin) of *Escherichia coli*. Biochem Biophys Acta 551:238–247. https://doi.org/10.1016/0005-2736(89)90002-3

Boonserm P, Davis P, Ellar DJ, Li J (2005) Crystal structure of the mosquito-larvicidal toxin Cry4Ba and its biological implications. J Mol Biol 348:363–382. https://doi.org/10.1016/j.jmb.2005.02.013

Boonserm P, Mo M, Angsuthanasombat C, Lescar J (2006) Structure of the functional from of the mosquito larvicidal Cry4Aa toxin from *Bacillus thuringiensis* at a 2.8-angstorm resolution. J Bacteriol 188:3391–3401. https://doi.org/10.1128/JB.188.9.3391-3401.2006

Chakraborty T, Schmid A, Notermans S, Benz R (1990) Aerolysin of *Aeromonas sobria*: evidence for formation of ion-permeable channels and comparison with alpha-toxin of *Staphylococcus aureus*. Infect Immun 58:2127–2132

Cohen S, Albeck S, Ben-Dov E, Cahan R, Firer M, Zaritsky A, Dym O (2011) Cyt1Aa toxin: crystal structure reveals implications for its membrane-perforating function. J Mol Biol 413:804–814. https://doi.org/10.1016/j.jmb.2011.09.021

Crickmore N, Bone EJ, Williams JA, Ellar DJ (1995) Contribution of the individual components of the δ-endotoxin crystal to the mosquitocidal activity of *Bacillus thuringiensis* subsp. *israelensis*. FEMS Microbiol Lett 131:249–254. https://doi.org/10.1111/j.1574-6968.1995.tb07784.x

de Maagd RA, Bravo A, Crickmore N (2001) How *Bacillus thuringiensis* has evolved specific toxins to colonize the insect world. Trends Genet 17:193–199. https://doi.org/10.1016/S0168-9525(01)02237-5

Fernández LE, Pérez C, Segovia L, Rodríguez MH, Gill SS, Bravo A, Soberón M (2005) Cry11Aa toxin from *Bacillus thuringiensis* binds its receptor in *Aedes aegypti* mosquito larvae through loop alpha-8 of domain II. FEBS Lett 579:3508–3514. https://doi.org/10.1016/j.febslet.2005.05.032

Georghiou GP, Wirth MC (1997) Influence of exposure to single versus multiple toxins of *Bacillus thuringiensis* subsp. *israelensis* on development of resistance in the mosquito *Culex quinquefasciatus* (Diptera: Culicidae). Appl Environ Microbiol 63:1095–1101

Grochulski P, Masson L, Borisova S, Pusztai-Carey M, Schwartz JL, Brousseau R, Cygler M (1995) *Bacillus thuringiensis* CryIA(a) insecticidal toxin: crystal structure and channel formation. J Mol Biol 254:447–464. https://doi.org/10.1006/jmbi.1995.0630

Hayakawa T, Kanagawa R, Kotani Y, Kimura M, Yamagiwa M, Yamane Y, Takebe S, Sakai H (2007) Parasporin-2Ab, a newly isolated cytotoxic crystal protein from *Bacillus thuringiensis*. Curr Microbiol 55:278–283. https://doi.org/10.1007/s00284-006-0351-8

Hayakawa T, Sakakibara A, Ueda S, Azuma Y, Ide T, Takebe S (2017) Cry46Ab from *Bacillus thuringiensis* TK-E6 is a new mosquitocidal toxin with aerolysin-type architecture. Insect Biochem Mol Biol 87:100–106. https://doi.org/10.1016/j.ibmb.2017.06.015

Ito A, Sasaguri Y, Kitada S, Kusaka Y, Kuwano K, Masutomi K, Mizuki E, Akao T, Ohba M (2004) A *Bacillus thuringiensis* crystal protein with selective cytocidal action to human cells. J Biol Chem 279:21282–21286. https://doi.org/10.1074/jbc.M401881200

Knapp O, Stiles B, Popoff MR (2010) The aerolysin-like toxin family of cytolytic, pore-forming toxins. Open Toxinol J 3:53–68. https://doi.org/10.2174/1875414701003020053

Knowles BH, Ellar DJ (1987) Colloid-osmotic lysis is a general feature of the mechanism of action of *Bacillus thuringiensis* δ-endotoxins with different insect specificity. Biochim Biophys Acta 924:509–518. https://doi.org/10.1016/0304-4165(87)90167-X

Likitvivatanavong S, Aimanova KG, Gill SS (2009) Loop residues of the receptor binding domain of *Bacillus thuringiensis* Cry11Ba toxin are important for mosquitocidal activity. FEBS Lett 583:2021–2030. https://doi.org/10.1016/j.febslet.2009.05.020

Melton JA, Parker MW, Rossjohn J, Buckley JT, Tweten RK (2004) The identification and structure of the membrane-spanning domain of the *Clostridium septicum* alpha toxin. J Biol Chem 279:14315–14322. https://doi.org/10.1074/jbc.M313758200

Pérez C, Fernandez LE, Sun J, Folch JL, Gill SS, Soberón M, Bravo A (2005) *Bacillus thuringiensis* subsp. *israelensis* Cyt1Aa synergizes Cry11Aa toxin by functioning as a membrane-bound receptor. Proc Natl Acad Sci USA 102:18303–18308. https://doi.org/10.1073/pnas.0505494102

Petit L, Maier E, Gibert M, Popoff MR, Benz R (2001) *Clostridium perfringens* epsilon toxin induces a rapid change of cell membrane permeability to ions and forms channels in artificial lipid bilayers. J Biol Chem 276:15736–15740. https://doi.org/10.1074/jbc.M010412200

Poncet S, Delécluse A, Klier A, Rapoport G (1995) Evaluation of synergistic interactions among the CryIVA, CryIVB, and CryIVD toxic components of *B. thuringiensis* subsp. *israelensis* crystals. J Invertebr Pathol 66:131–135. https://doi.org/10.1006/jipa.1995.1075

Puntheeranurak T, Uawithya P, Potvin L, Angsuthanasombat C, Schwartz JL (2004) Ion channels formed in planar lipid bilayers by the dipteran-specific Cry4B *Bacillus thuringiensis* toxin and its alpha1–alpha5 fragment. Mol Membr Biol 21:67–74. https://doi.org/10.1080/09687680310001625792

Schnepf E, Crickmore N, Van Rie J, Lereclus D, Baum J, Feitelson J, Zeigler DR, Dean DH (1998) *Bacillus thuringiensis* and its pesticidal crystal proteins. Microbiol Mol Biol Rev 62:807–813

Schwartz JL, Garneau L, Savaria D, Masson L, Brousseau R, Rousseau E (1993) Lepidopteran-specific crystal toxins from *Bacillus thuringiensis* form cation- and anion-selective channels in planar

lipid bilayers. J Membr Biol 132:53–62. https://doi.org/10.1007/BF00233051

Shai Y, Bach D, Yanovsky A (1990) Channel formation properties of synthetic pardaxin and analogues. J Biol Chem 265:20202–20209

Sher D, Fishman Y, Zhang M, Lebendiker M, Gaathon A, Mancheño JM, Zlotkin E (2005) Hydralysins, a new category of β-pore-forming toxins in Cnidaria. J Biol Chem 280:22847–22855. https://doi.org/10.1074/jbc.M503242200

Slatin SL, Abrams CK, English L (1990) Delta-endotoxins form cation-selective channels in planar lipid bilayers. Biochem Biophys Res Commun 169:765–772. https://doi.org/10.1016/0006-291X(90)90397-6

Tabashnik BE, Cushing NL, Finson N, Johanson MW (1990) Field development of resistance of *Bacillus thuringiensis* in diamondback moth (Lepidoptera: Plutellidae). J Econ Entomol 83:1671–1676. https://doi.org/10.1093/jee/83.5.1671

Von Tersch MA, Slatin SL, Kulesza CA, English LH (1994) Membrane-permeabilizing activities of *Bacillus thuringiensis* coleopteran-active toxin CryIIIB2 and CryIIIB2 domain I peptide. Appl Environ Microbiol 60:3711–3717

Wirth MC, Georghiou GP, Federici BA (1997) CytA enables CryIV endotoxins of *Bacillus thuringiensis* to overcome high levels of CryIV resistance in the mosquito, *Culex quinquefasciatus*. Proc Natl Acad Sci USA 94:10536–10540. https://doi.org/10.1073/pnas.94.20.10536

Wirth MC, Park HW, Walton WE, Federici BA (2005) Cyt1A of *Bacillus thuringiensis* delays evolution of resistance to Cry11A in the mosquito *Culex quinquefasciatus*. Appl Environ Microb 71:185–189. https://doi.org/10.1128/AEM.71.1.185-189.2005

Wirth MC, Walton WE, Federici BA (2012) Inheritance, stability, and dominance of cry resistance in *Culex quinquefasciatus* (Diptera: Culicidae) selected with the three cry toxins of *Bacillus thuringiensis* subsp. *israelensis*. J Med Entomol 49:886–894

Wu D, Johnson JJ, Federici BA (1994) Synergism of mosquitocidal toxicity between CytA and CryIVD proteins using inclusions produced from cloned genes of *Bacillus thuringiensis*. Mol Microbiol 13:965–972. https://doi.org/10.1111/j.1365-2958.1994.tb00488.x

Xu C, Wang BC, Yu Z, Sun M (2014) Structural insights into *Bacillus thuringiensis* Cry, Cyt and parasporin toxins. Toxins (Basel) 6:2732–2770. https://doi.org/10.3390/toxins6092732